Inorg. Chem. **2004**, *43*, 1885–1894

Diastereoselective Assembling of 21-C-Alkylated Nickel(II) Complexes of Inverted Porphyrin on a Platinum(II) Template

Piotr J. Chmielewski* and Izabela Schmidt

Department of Chemistry, University of Wrocław F. Joliot-Curie Street 14, 50 383 Wrocław, Poland

Received October 7, 2003

Reaction of 21-C-methyl and 21-C-benzyl nickel(II) complexes of inverted *meso*-tetratolylporphyrin with platinum(II) dichloride or its bis(benzonitrile) complex yields a chloroplatinum(II) species containing two nickel(II) carbaporphyrinoids in a cis arrangement. One of the carbaporphyrinoids coordinates to the platinum ion with the external nitrogen while the other is bound with the external nitrogen and one *ortho*-carbon of the adjacent *meso*-aryl ring. The reaction is highly chemoselective. ^{1}H and ^{13}C NMR experiments in solution show the diastereoselectivity of the reaction. Single-crystal X-ray data confirm the presence of the diastereomer with opposite configurations of the Ni(II)-coordinated carbons in the subunits of the dimer. Cyclovoltammetric measurements reveal an anodic shift of the nickel(II) oxidation potentials of dimers with respect to those of the parent monomers and two different reduction couples. Reaction of unsubstituted inverted porphyrin with $Pt(PhCN)_2Cl_2$ in chlorobenzene yields a monomeric platinum(II) complex of inverted porphyrin. This complex displays a markedly upfield ^{195}Pt NMR shift compared to tetraphenylporphyrinatoplatinum(II). Under strongly basic conditions deprotonation of the external nitrogen of inverted porphyrin and both electrochemical and chemical oxidation of platinum(II) center are observed.

Introduction

Porphyrins and metalloporphyrins provide an attractive class of building blocks for the construction of large multicomponent 2D and 3D molecular arrays, which are being considered as possible biomimetic models, catalysts, and materials for the transport of charge, molecules, and ions. Both covalent[1,2] and coordination linkages[3−11] have been exploited in the design of a variety of discrete porphyrin or porphyrazin assemblies. The supramolecular approach based on intermolecular interactions of appropriately selected peripheral functionalities is particularly promising, though it requires well-planned substitution either at β-pyrrole or *meso*-positions of the porphyrin.

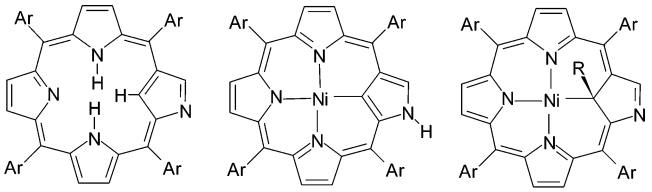

Inverted porphyrin **1**[12,13] and some of its derivatives[14−17] and complexes[18−20] possess the external nitrogen of the

* Author to whom correspondence should be addressed. Fax: (48 71) 32 823 48. Tel: (48 71) 37 57 277. E-mail: pjc@wchuwr.chem.uni.wroc.pl.

(1) Burrell, A. K.; Officer, D. L.; Plieger, P. G.; Reid, D. C. W. *Chem. Rev.* **2001**, *101*, 2751−2796.
(2) Jeandon, C.; Ruppert, R.; Richeter, S.; Callot, H. J. *Org. Lett.* **2003**, *5*, 1487.
(3) Wojaczyński, J.; Latos-Grażyński, L. *Coord. Chem. Rev.* **2000**, *204*, 113.
(4) Richeter, S.; Jeandon, C.; Ruppert, R.; Callot, H. J. *Chem. Commun.* **2001**, 91.
(5) Richeter, S.; Jeandon, C.; Sauber, C.; Gisselbrecht, J.-P.; Ruppert, R.; Callot, H. J. *J. Porphyrins Phthalocyanines* **2002**, *6*, 423.
(6) Richeter, S.; Jeandon, C.; Gisselbrecht, J.-P.; Ruppert, R.; Callot, H. J. *J. Am. Chem. Soc.* **2002**, *124*, 6.
(7) Richeter, S.; Jeandon, C.; Ruppert, R.; Callot, H. J. *Chem. Commun.* **2002**, 266.
(8) Michel, S. L. J.; Barret, A. G. M.; Hoffman, B. M. *Inorg. Chem.* **2003**, *42*, 814.
(9) Sakellariou, E. G.; Montablau, A. G.; Meunier, H. G.; Rumbles, G.; Phillips, D.; Ostler, R. B.; Suhling, K.; Barret, A. G. M.; Hoffman, B. M. *Inorg. Chem.* **2002**, *41*, 2182.
(10) Deng, K. M.; Ding, Z. N.; Ellis, D. E.; Michel, S. L. J.; Hoffman, B. M. *Inorg. Chem.* **2001**, *40*, 1110.
(11) Zhao, M.; Stern, C.; Barret, A. G. M.; Hoffman, B. M. *Angew. Chem., Int. Ed.* **2003**, *42*, 462.
(12) Chmielewski, P. J.; Latos-Grażyński, L.; Rachlewicz, K.; Głowiak, T. *Angew. Chem., Int. Ed. Engl.* **1994**, *33*, 779.
(13) Furuta, H.; Asano, T.; Ogawa, T. *J. Am. Chem. Soc.* **1994**, *116*, 767.
(14) Schmidt, I.; Chmielewski, P. J. *Tetrahedron Lett.* **2001**, *42*, 1151.
(15) Schmidt, I.; Chmielewski, P. J. *Tetrahedron Lett.* **2001**, *42*, 6389.

10.1021/ic035162l CCC: $27.50
Published on Web 02/21/2004

inverted pyrrole, which can act as a donor site.[21−23] Several dimeric structures of the inverted porphyrin complexes have been reported recently, where the external nitrogen is coordinated either to the metal ion in the macrocyclic crevice of the other subunit (Mn(II), Fe(II), Zn(II)) or to the extraneous bridging cation (Zn(II)).[24−26] In all those systems, however, the protonated internal carbon of the inverted pyrrole has been only weakly involved in the side-on π-coordination to the metal ion.

In the case of nickel(II) complex **2**, where internal carbon forms a σ-bond with the metal ion, protonation of the external nitrogen prevents it from coordinating a metal ion.[12] Under strongly basic conditions we observed a dimerization with a bridging potassium ion in solution.[27] Methylation on the internal carbon (C21) of the inverted pyrrole in the nickel(II) complexes also leads to deprotonation of the external nitrogen retaining strong coordination of the pyramidal C21.[18] As we have shown recently, alkylation of this donor site gives a variety of modified monomeric and dimeric derivatives.[27−29] Here we show that they can be applied as chiral building blocks of larger molecular systems.

Results and Discussion

Synthesis and Spectroscopic Characterization. Reaction of 5,10,15,20-tetrakis(*p*-tolyl)-21-methyl-2-aza-21-carbaporphyrinato nickel(II) (**3**) or 5,10,15,20-tetrakis(*p*-tolyl)-21-benzyl-2-aza-21-carbaporphyrinato nickel(II) (**4**) with $PtCl_2$ in refluxing chloroform, in the presence of potassium carbonate as a proton scavenger, yields after 24 h the unsymmetrical dimeric species **5** or **6**, respectively. Platinum(II) bis-benzonitrile dichloride can also be used as an alternative metal ion carrier of superior solubility. Application of $Pt(PhCN)_2Cl_2$ is particularly useful for the experiments where permanent excess of platinum(II) over the nickel(II) complex in solution has to be maintained. We do not observe any particular dependence of the reaction yield or rate on the applied platinum(II) ion source or its amount in solution (up to a 10-fold excess). It is in contrast with the reaction of inverted porphyrin free base, for which the yield of dimeric species strongly depended on the platinum(II) to porphyrin molar ratio.[23] The coordination process is highly chemoselective with respect to the asymmetric dimer since we detect the formation of only traces of other species for both complexes despite an excess of available platinum in the reaction mixture, irrespective of the reaction time (from 6 to 70 h).

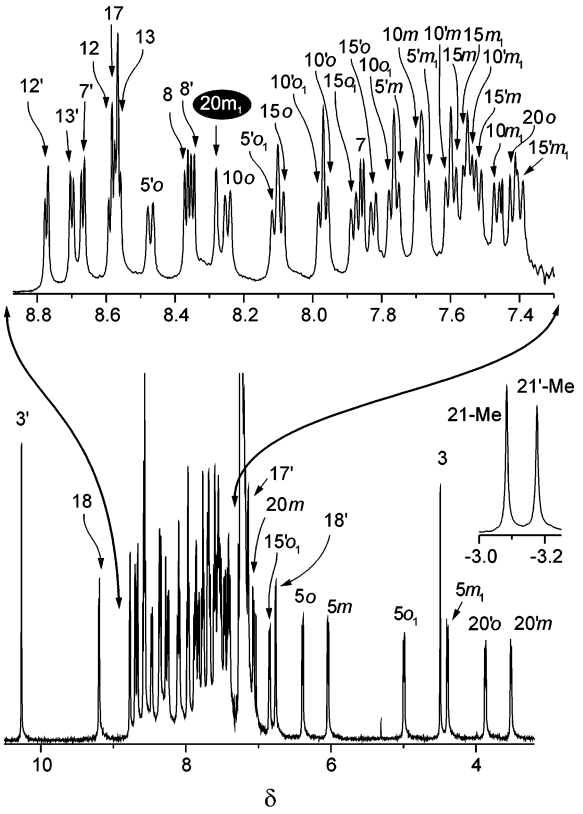

Figure 1. Low- and high-field fragments of the 500 MHz ^{1}H NMR spectrum of **5** in $CDCl_3$, 213 K.

Mass spectrometry (MALDI TOF) confirms the presence of two metalloporphyrinoid units, platinum, and chloride in **5** and **6** while ^{1}H and ^{13}C NMR data afford definitive structural information.

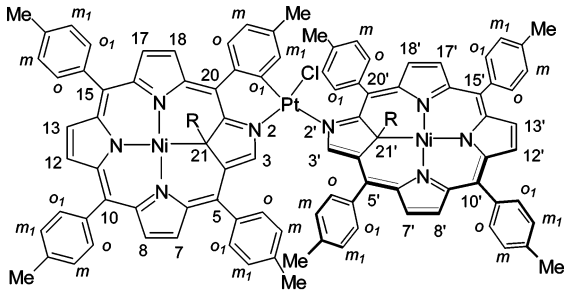

5: R = Me
6: R = CH_2Ph

The asymmetric character of **5** and **6** is revealed by the ^{1}H NMR spectra where two sets of pyrrole and 21-alkyl signals can be observed (Figure 1). These spectra are rather complex due to inherent asymmetry of the subunits of the dimer as well as restriction in a rotational freedom of each of the *meso*-aryl rings at low temperature (213 K). The assignments of the resonances in ^{1}H NMR and ^{13}C spectra are based on homo- and heteronuclear correlation techniques (COSY, NOESY, ROESY, ^{1}H−^{13}C HMQC, ^{1}H−^{13}C HMBC).

(16) Ishikawa, Y.; Yoshida, I.; Akaiwa, K.; Koguchi, E.; Sasaki, T.; Furuta, H. *Chem. Lett.* **1997**, 453.
(17) Furuta, H.; Maeda, H.; Osuka, A. *J. Am. Chem. Soc.* **2000**, *122*, 803.
(18) Chmielewski, P. J.; Latos-Grażyński, L.; Głowiak, T. *J. Am. Chem. Soc.* **1996**, *118*, 5690.
(19) Furuta, H.; Ogawa, T.; Uwatoko, Y.; Araki, K. *Inorg. Chem.* **1999**, *38*, 2676.
(20) Ogawa, T.; Furuta, H.; Takahashi, M.; Morino, A.; Uno, H. *J. Organomet. Chem.* **2000**, *611*, 551.
(21) Furuta, H.; Kubo, N.; Maeda, H.; Ishizuka, T.; Osuka, A.; Nanami, H.; Ogawa, T. *Inorg. Chem.* **2000**, *39*, 5424.
(22) Srinivasan, A.; Furuta, H.; Osuka, A. *Chem. Commun.* **2001**, 1666.
(23) Furuta, H.; Youfu, K.; Maeda, H.; Osuka, A. *Angew. Chem., Int. Ed.* **2003**, *42*, 2186.
(24) Harvey, J. D.; Ziegler, C. J. *Chem. Commun.* **2002**, 1942.
(25) Hung, C.-H.; Chen, W.-C.; Lee, G.-H.; Peng, S.-M. *Chem. Commun.* **2002**, 1516.
(26) Furuta, H.; Ishizuka, T.; Osuka, A. *J. Am. Chem. Soc.* **2002**, *124*, 5622.
(27) Schmidt, I.; Chmielewski, P. J.; Ciunik, Z. *J. Org. Chem.* **2002**, *67*, 8917.
(28) Schmidt, I.; Chmielewski, P. J. *Chem. Commun.* **2002**, 92.
(29) Schmidt, I.; Chmielewski, P. J. *Inorg. Chem.* **2003**, *42*, 5579.

The procedure of peak assignment starts from identification of the most characteristic signals in both subunits of the dimer. 3-H and 3′-H are assigned on the basis of their long-range coupling with quaternary aliphatic 21-C and 21′-C which in turn correlate with upfield-shifted alkyl protons (CH_3 or CH_2-Ph) in the HMBC spectrum. The 3 and 3′ protons are in contact with 5-*o* and 5′-*o*, respectively, which can be observed in the NOESY and ROESY experiments. The chemical exchange-type correlations of the latter protons in the ROESY map allow assignment of the 5-o_1 and 5′-o_1 signals. The resonances of the *meta* protons were identified on the basis of the scalar couplings giving cross-peaks in the COSY with respective *ortho* protons. Further steps of the assignment procedure involve analysis of the contacts between *ortho* and the neighboring β-pyrrole protons and scalar couplings of the protons belonging to the same pyrrole and between vicinal *ortho* and *meta* protons of each aryl ring. The *ortho* or *meta* protons of a particular aryl ring which have opposite orientations with respect to the normal to the average porphyrin plane (i.e. *o* and o_1 or *m* and m_1 aryl protons in all *meso* positions except position 20) display chemical exchange-related cross-peaks in the NOESY and ROESY correlation map. Most of these proton pairs are also scalar coupled, which can be observed in the COSY experiments. The *para*-methyl substituents can be assigned to the particular *meso*-aryl ring based both on the contacts and on the scalar couplings with the appropriate *meta* protons.

Coordination of the platinum(II) dication to the external nitrogen atoms of inverted pyrroles is expected to introduce additional positive charge to the system, analogously as in the case of protonation, which led to the formation of paramagnetic species.[18,28,29] However, the diamagnetic character of the dimer indicates lack of coordination of an apical anionic ligand to the nickel(II) centers. Coordination of one chloride ion to the platinum(II) partially compensates the additional charge. The other part is neutralized by coordination of deprotonated *ortho*-carbon of the tolyl ring bound in the *meso*-position 20 in the vicinity of the coordinated external nitrogen (20o_1). Such an orthometalation has been observed previously for inverted porphyrin dimers linked by palladium(II)[21] and platinum(II).[23] The spectral feature diagnostic for such a coordination mode of one of the porphyrinoid subunits is a signal appearing in the ^{1}H NMR spectrum at 8.37 ppm (**5**, $CDCl_3$, 298 K). This signal is assigned to the *meta* proton 20m_1. Unlike in the case of the other *meta* protons, for this proton only a scalar coupling with 20*m* ($^4J = 1.8$ Hz) and a correlation with the appropriate *para*-methyl protons (at 2.40 ppm) in the COSY and NOESY experiments can be observed. There is neither a vicinal coupling of 20m_1 to an *ortho* proton (with an expected coupling constant about 7 Hz) nor a chemical-exchange correlation with 20*m* in the ROESY experiment. This indicates that no proton is present in the position 20o_1 and the rotation of the ring is frozen. Analogous spectral features are observed for **6**.

The integrity of the molecule in solution and the close contact of the porphyrinoid subunits can be inferred from the strong upfield shift of some signals in the ^{1}H NMR spectra. In particular, the resonance of 3-H appears at about 4.5 ppm, which indicates a strong shielding influence of the aromatic ring current since in monomeric precursors **3** or **4** this proton resonates at about 9.7 ppm.[18,29] The proton in position 3′ is deshielded by the neighboring aromatic ring since its signal is shifted downfield (ca. 0.5 ppm) with respect to the parent monomer. Significantly, protons 3 and 3′ give correlations in the NOESY and ROESY experiments indicating a *cis*-configuration of the porphyrinoid subunits around the platinum(II) center.

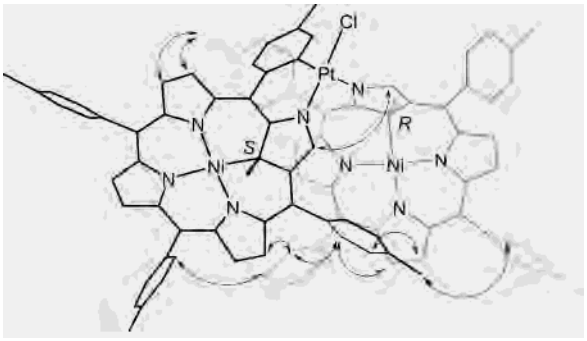

Figure 2. Molecular model of **5** (based on ^{1}H−^{1}H contacts indicated by arrows) showing arrangement of porphyrinoid fragments and configurations of the asymmetric carbons in one of the enantiomers.

Also the remaining through-space contacts between protons belonging to the different parts of the dimer can be exploited for establishing of average mutual orientation of the carbaporphyrin subunits of the complex in solution. The NOE correlations ($CDCl_3$, 213 K) between protons of the *para*-methyl group of the tolyl substituent in position 20′ (1.93 ppm) with 17-H and 18-H (8.57 and 9.19 ppm, respectively), i.e. β-pyrrole protons belonging to the other part of the molecule, as well as contacts between 5o_1, 5m_1, 12′, and 13′ indicate a partially eclipsed position of the macrocyclic rings. Some of the protons of the aryl rings in positions 5 and 20′, i.e. those in contact with the other fragment of the dimer, display strong high-field shifts in the ^{1}H NMR due to the shielding influence of the aromatic ring current of the neighboring porphyrin ring. Signals of both *ortho* and *meta* protons of these aryls cannot be observed at room temperature due to broadening caused by a chemical exchange related to the rotation of these rings. The methyl signal of the *para*-tolyl substituent in position 5 is shifted up to 1.23 ppm, i.e. more than 1 ppm upfield with respect to the average chemical shift of other methyl signals. It again indicates a shielding effect of the aromatic ring current and corresponds to a position of the methyl group above the plane of the carbaporphyrinoid moiety.

The assignment of the resonances and analysis of the respective chemical shifts, scalar ^{1}H−^{1}H and multibond ^{1}H−^{13}C couplings as well as ^{1}H−^{1}H through-space contacts allows the construction of a reliable molecular model (Figure 2).

The molecule of **5** or **6** possesses two different stereogenic centers (C21 and C21′) that are rigidly linked and relatively close to each other. Two pairs of diastereotopic methylene proton signals in the high-field region of the ^{1}H NMR spectrum of **6** reflect the presence of two different asym-

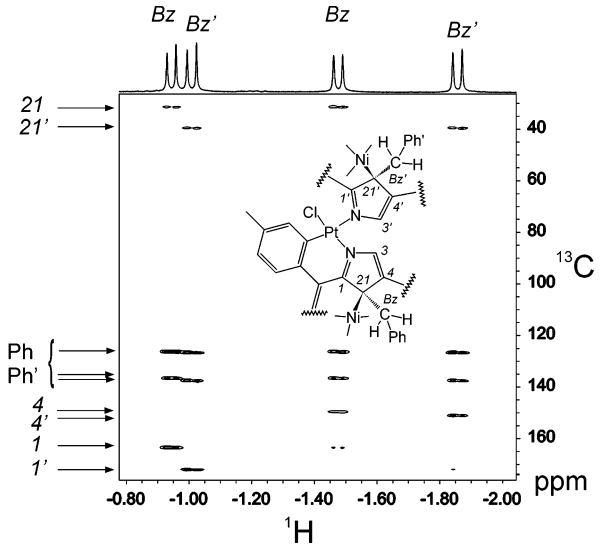

Figure 3. A fragment of a $^1H-^{13}C$ HMBC map of **6** ($CDCl_3$, 298 K) showing diastereotopic differentiation of methylene protons (*Bz* and *Bz*′) of benzyl substituents and their long-range coupling with carbons assigned on the graph.

metric carbons (Figure 3). The racemic mixtures of starting complexes **3** or **4** are applied; thus formation of two NMR-distinguishable diastereomers is possible. Since only one form of **5** or **6** is observed, we conclude that coordination to the platinum ion is diastereoselective. The molecular model presented above suggests that only the structures of *RS* and *SR* enantiomers are consistent with the ^1H NMR results. The stereoselectivity is presumably due to the rigid square-planar geometry of the platinum(II) environment, *cis*-configuration of the complex, and presence of aryl substituents in the vicinity of the platinum(II) center. In addition, the presence of methyl or benzyl substituents on the C21 and C21′ favors such a mutual arrangement of the porphyrin faces in which the 21-substituents are on the opposite sides of the porphyrin planes.

The diastereoselective assembling of the metalloporphyrin units has been observed previously for the iron(III), gallium(III), or manganese(III) β-hydroxy-substituted tetraphenylporphyrin forming coordinatively linked cyclic trimers.[30−32]

The electronic spectra of **5** and **6** are similar to those of monomeric precursors **3** and **4**, respectively, except for a broad feature near the major absorption band observed for the dimers (Figure 4). This indicates little change in the electronic structure of the macrocyclic fragments upon coordination of the external nitrogen to platinum(II). Protonation of the external nitrogen apparently causes a more pronounced alteration of the electronic spectrum which can be accounted for by changes in the spin state and coordination number of nickel(II) center on going from **3** to **3**-HCl or from **4** to **4**-HCl.[18,29]

X-ray Structure of 6. The single-crystal X-ray analysis performed for **6** reveals an asymmetric dimeric structure of

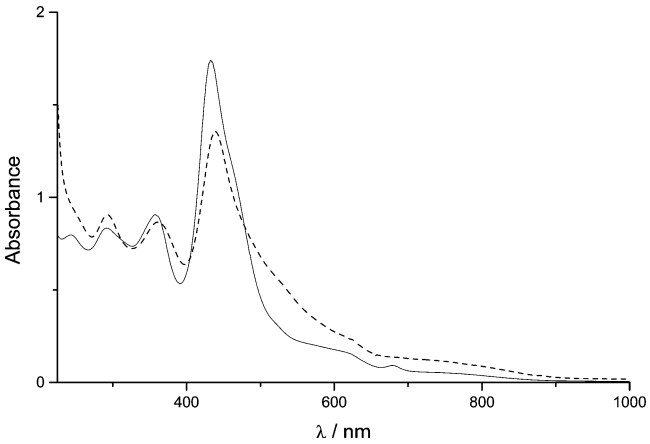

Figure 4. Optical spectra of **4** (solid line) and **6** (dashed line) in CH_2Cl_2.

the complex and supplies further details concerning mutual arrangement of the carbaporphyrin subunits and chloroplatinum template in the solid state (Figure 5). The *cis*-configuration of the porphyrinoids coordinated around the platinum(II) and the orthometalation of one of them are evident. The structural features characteristic of the 21-alkylated nickel(II) complexes of inverted porphyrins[18] are retained in both parts of the dimer. The lack of an apical ligand in the environment of the nickel(II) centers and roughly planar arrangement of both NiCNNN fragments is consistent with the diamagnetism of the dimer. The geometry of internal carbons (C21 and C21′) can be deduced from the sums of bond angles around the coordinated carbons, i.e. from the values of Σ_1 = Ni−C21−C1 + Ni−C21−C4 + Ni−C21−C(benzyl) and Σ_2 = C1−C21−C4 + C1−C21−C(benzyl) + C4−C21−C(benzyl). These sums should both equal 328.5° for an idealized tetrahedral geometry, but 270° and 360°, respectively for the p_z side-on coordination of the inverted pyrrole.[18] In **6**, Σ_1 = 331(3)° and Σ_2 = 327(4)° for C21 and Σ_1 = 322(3)° and Σ_2 = 335(4)° for C21′ (C21A in Figure 5), indicating a pyramidal geometry of the coordinated carbons. This is in line with their chemical shifts in ^{13}C NMR (31.1 ppm for C21 and 39.9 ppm for C21′, **6**, $CDCl_3$, 233 K) typical of the sp^3 carbons. The configurations at C21 and C21A are opposite; thus the X-ray data of **6** unequivocally show the presence of the *RS*/*SR* diastereomer in the solid state. The inverted pyrroles in both parts of the dimer are essentially planar with 0.01 or 0.02 Å mean deviations from the planes defined by all five ring atoms in the orthometalated or non-orthometalated fragment, respectively. In both fragments of the dimer these pyrroles are tilted out of the mean planes defined by nickel and atoms coordinated to it. The dihedral angle between planes defined by inverted pyrrole and the NiCNNN plane is 34° for orthometalated and 41° for the non-orthometalated part. The deviations of the coordinated atoms in the platinum atom environment from the Pt1−N2−N2A-Cl1−C47 plane are about −0.12 Å for N2 and Cl1 and 0.14 Å for N2A and C47. None of the rings coordinated to the platinum is coplanar with this plane. The dihedral angles between that plane and inverted pyrroles or coordinated tolyl are as follows: N2−C3−C1−C4−C21, 34°; N2A−C3A−C1A−C4A−C21A, 61°; C46−C47−C48−

(30) Wojaczyński, J.; Latos-Grażyński, L. *Inorg. Chem.* **1995**, *34*, 1044.
(31) Wojaczyński, J.; Latos-Grażyński, L. *Inorg. Chem.* **1995**, *34*, 1054.
(32) Wojaczyński, J.; Latos-Grażyński, L. *Inorg. Chem.* **1996**, *35*, 4812. Wojaczyński, J.; Latos-Grażyński, L.; Olmstead, M. M.; Balch, A. L. *Inorg. Chem.* **1997**, *36*, 4548.

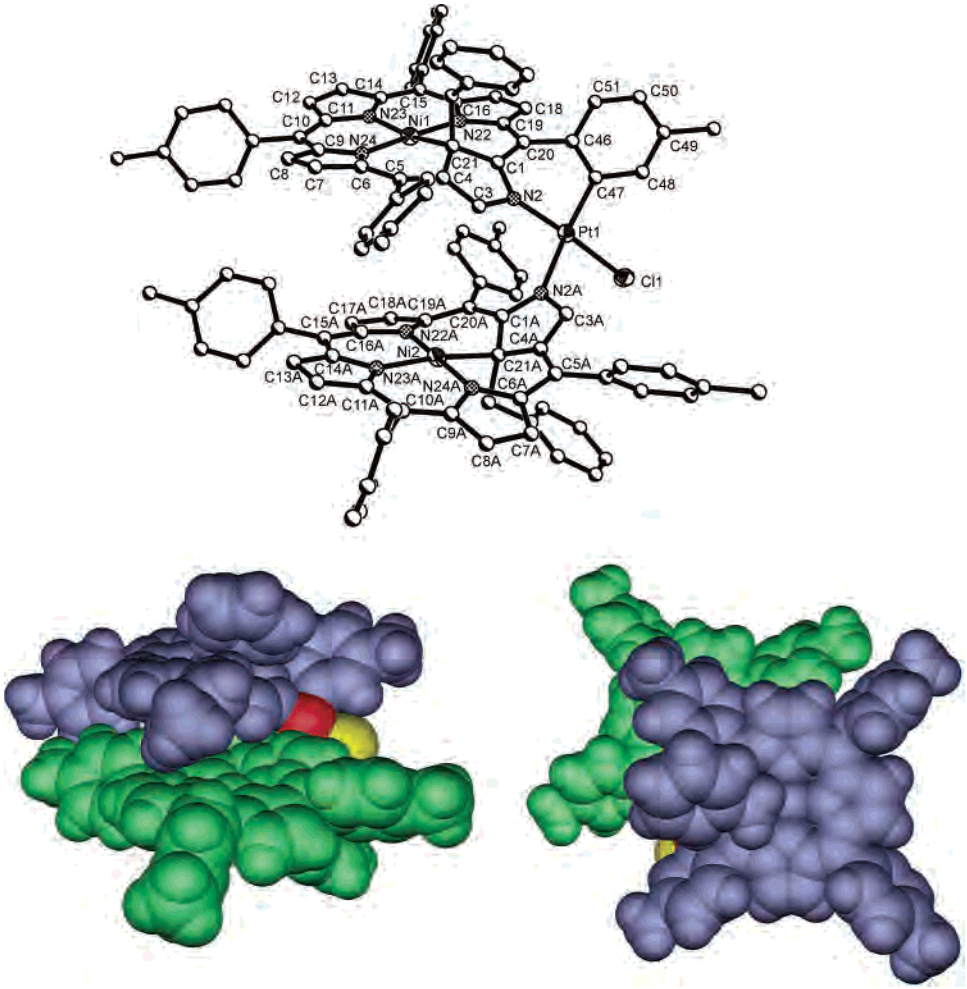

Figure 5. Perspective view (top, all hydrogen atoms are omitted) and space-filling representations (bottom) of **6** (the 21-*S*,21A-*R* enantiomer). Selected bond lengths (Å) and angles (deg) and torsion angles (deg): Pt1−N2, 1.92(1); Pt1−N2A, 2.11(1); Pt1−Cl1, 2.311(5); Pt1−C47, 2.01(2); Ni1−N23, 1.95(1); Ni1−N24, 1.98(1); Ni1−N22, 1.98(1); Ni1−C21, 2.03(1); Ni2−C21A, 2.09(2); Ni2−N23A, 1.92(1); Ni2−N24A, 1.94(1); Ni2−N22A, 1.95(1); N2−Pt1−C47, 88.5(8); N2−Pt1−N2A, 94.1(6); C47−Pt1−N2A, 169.4(6); N2−Pt1−Cl1, 175.5(5); C47−Pt1−Cl1, 93.7(6); N2A−Pt1−Cl1, 84.5(4); N23−Ni1−N24, 91.3(6); N23−Ni1−N22, 92.8(6); N24−Ni1−N22, 175.9(6); N23−Ni1−C21, 168.8(6); N24−Ni1−C21, 87.5(6); N22−Ni1−C21, 88.5(6); N23A−Ni2−N24A, 91.9(6); N23A−Ni2−N22A, 91.3(6); N24A−Ni2−N22A, 174.1(6); N23A−Ni2−C21A, 171.4(6); N24A−Ni2−C21A, 87.0(6); N22A−Ni2−C21A, 89.1(6); Pt1−N2−C1−C20, −20(2); Pt1−C47−C46−C20, −1(2); Pt1−C47−C48−C49, −173(1); C1−C20−C46−C47, 35(2); N2−C1−C20−C46, −25(3); N2−Pt1−N2A−C3A, −121(1); C1A−N2A−Pt1−N2, 53(2).

C49−C50−C51, 31°. The dihedral angle between Pt1−N2−N2A−Cl1−C47 and either of the NiCNNN planes is close to 60° (59° for Ni1−C21−N22−N23−N24 and 58° for Ni2−C21A−N22A−N23A−N24A). On the other hand both planes containing nickel atoms are nearly parallel with a dihedral angle of 10° between them. The carbaporphyrinoid units overlap to some extent forming a shallow cleft. Such an arrangement is in agreement with the model deduced above on the basis of interprotonic contacts (Figure 2). In fact, the solid-state nonbonding distances between these protons belonging to the different parts of the dimer, for which a NOE correlation in solution is observed, are in a range of 2.5−3.2 Å. The one exception is a pair of protons bound to the carbon 3 and 3′ (3A in Figure 5) for which the estimated distance in the solid state is about 4 Å. On the other hand the dynamics of the molecule in solution, i.e. rotation around the Pt1−N2A bond, can markedly change this distance.

Due to the presence of the *meso*-tolyl rings the rotation around the Pt1−N2A bond is restricted. It can be shown on the model based on the crystal structure that the torsion angle C1A−N2A−Pt1−N2 (53(2)° for the solid-state structure) can vary from about 30° to 110°. At the values lower than 30° an unacceptable contact between the aryl ring bound to C20A and Ni1 would appear, while at the values higher than 110° the tolyl rings in the positions 5 and 5′ would collide. The nonbonding distance between protons 3 and 3′ varies from 2.3 to 4.4 Å on going from the high to low limit of the torsion angle C1A−N2A−Pt1−N2.

Dealkylation and Insertion of Platinum(II). Although **5** and **6** are stable in the presence of air even at elevated temperatures, both in the solid state and in solution, it seems that dealkylation of the nickel(II)-coordinated carbon can take place under certain conditions. The MALDI-TOF mass spectrum of **6** contains, apart from the molecular peak at 1864 amu, also fragmentation peaks showing loss of one and two benzyl substituents (1774 and 1682 amu, respectively). No such dealkylated fragments are observed for **5**. During the synthesis of **6**, a small fraction containing **2** (about 10% of the starting complex **4**) can be separated from the

reaction mixture when the process is carried out with an excess of $Pt(PhCN)_2Cl_2$ and no proton scavenger is present. Previously we observed such a dealkylation process for the N-protonated homologue of **4** in the presence of oxygen.[29] Thus the formation of **2** can be caused by HCl that is liberated upon orthoplatination.

There are several reports concerning C−C bond activation in solution of organometallic compounds mostly containing late transition elements of the second and third rows.[33−37] A detailed study on the dealkylation of regular porphyrins has been performed by Lavallee and co-workers for various complexes of divalent transition metal ions.[38] The mechanism of the dealkylation observed for 21-C-benzyl-substituted inverted porphyrin can be similar to that observed for the N-alkylated regular analogues.[39−43] Stabilization of intermediate carbocation in the case of the benzyl group evidently promoted dealkylation, which may reflect the S_N1 character of that process.

Formation of a protonated, paramagnetic complex **3**−HCl containing 5-coordinated nickel(II)[18] can be observed, apart from the desired dimer **5**, after refluxing **3** with a 2-fold excess of $Pt(PhCN)_2Cl_2$ in the absence of any proton scavenger (40 h, $CHCl_3$). The molar ratio of **3**−HCl to **5** is close to 50/50 as it can be estimated on the basis of the ^{1}H NMR spectrum of the crude reaction mixture.

Clearly, N-protonation with a concurrent chloride ligation to the Ni^{2+} is a competitive reaction to that of Pt^{2+} coordination to the external nitrogen in **3** or **4**. Also, our attempt to coordinate platinum(II) to the unsubstituted nickel(II) complex of inverted porphyrin **2** failed, likely due to presence of a proton on the potential donor 2-N.

In the case of inverted porphyrin free base **1** coordination to platinum(II) can take place either on the porphyrin perimeter or in the macrocyclic interior.[23] However, no product with both inner and outer coordination sites occupied by platinum(II) has been observed. It can also be related to a competition of the protonation and coordination/orthometalation reactions.

The effectiveness of the insertion of the platinum(II) ion into inverted porphyrin **1** depends on the reaction conditions. When chloroform is used as the solvent, formation of only traces of **7** is observed, even after 18 h of reflux with 3- to 5-fold excess of $Pt(PhCN)_2Cl_2$. The major product that can

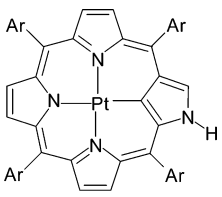

7a, Ar = Ph
7b, Ar = *p*-Tol

be isolated is an asymmetric dimer, analogous to that reported by Furuta et al.[23] that we identified by ^{1}H NMR and MALDI-TOF mass spectrometry (1572 amu). On the other hand, when reaction is carried out in chlorobenzene with an excess of $Pt(PhCN)_2Cl_2$, the monomeric complex **7** can be obtained

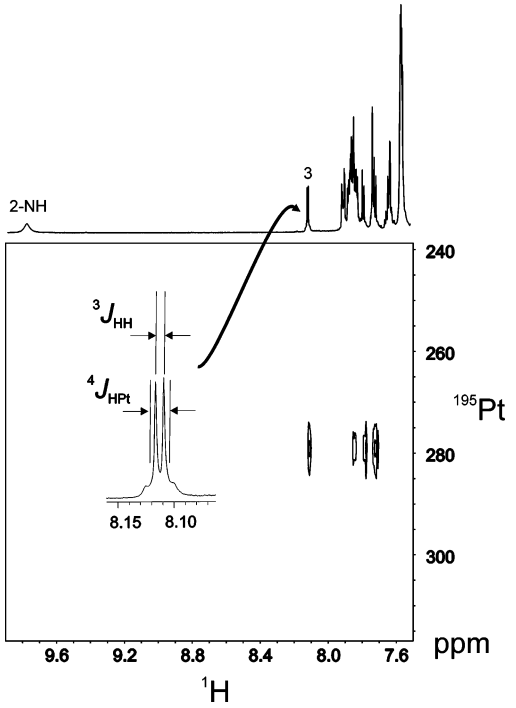

Figure 6. ^{1}H NMR spectrum and ^{1}H−^{195}Pt HMBC correlation map of **7a** ($CDCl_3$, 333 K). The inset shows expansion of the signal of 3-H with platinum satellites marked.

in high yield. The ^{1}H NMR spectrum of **7** contains features similar to those observed for nickel(II)[12] and palladium(II)[21] complexes of that type, i.e. a low field 2-NH signal (Ar = Ph, 9.92 ppm, **7a**, $CDCl_3$, 298K) and a doublet of 3-H (8.16 ppm). However, certain signals of pyrrole protons are accompanied by satellites, which are rather broad but can be observed, particularly at higher temperature (333 K). These features are due to multibond heteronuclear ^{1}H−^{195}Pt coupling ($^4J_{HPt}$ = 8.9 Hz for 3-H in **7a**) which can be confirmed by a HMBC experiment (Figure 6). Similar spectral features have been reported recently for the related platinum(II) complex of azuliporphyrin.[44] The ^{195}Pt resonance of **7** (280 ppm) is strongly shifted upfield relative to that of [(TPP)Pt^{II}] (1235 ppm),[45] which may reflect the presence of a different donor in the coordination core. On the other hand, for **7** this resonance appears at significantly higher field than

(33) Milstein, D.; Rybtchinski, B. *Angew. Chem., Int. Ed. Engl.* **1999**, *38*, 870.
(34) Rybtchinski, B.; Oevers, S.; Montag, M.; Vigalok, A.; Rozenberg, H.; Martin, J. M. L.; Milstein, D. *J. Am. Chem. Soc.* **2001**, *123*, 9064.
(35) Sundermann, A.; Uzan, O.; Milstein, D.; Martin, J. M. L. *J. Am. Chem. Soc.* **2000**, *122*, 7095.
(36) Albrecht, M.; Gossage, R. A.; Spek, A. L.; van Koten, G. *J. Am. Chem. Soc.* **1999**, *121*, 11898.
(37) Gandelman, M.; Shimon, L. J. W.; Milstein, D. *Chem. Eur. J.* **2003**, *9*, 4295.
(38) Lavallee, D. K. *The Chemistry and Biochemistry of N-substituted Porphyrins*; VCH Publishers: New York, 1987.
(39) Lavallee, D. K. *Inorg. Chem.* **1976**, *15*, 691.
(40) Lavallee, D. K. *Inorg. Chem.* **1977**, *16*, 955.
(41) Kuila, D.; Lavallee, D. K. *Inorg. Chem.* **1983**, *22*, 1095.
(42) Lavallee, D. K.; Kuila, D. *Inorg. Chem.* **1983**, *22*, 3987.
(43) Doi, J. D.; Compito-Magliozzo, C.; Lavallee, D. K. *Inorg. Chem.* **1984**, *23*, 79.
(44) Lash, T. D.; Colby, D. A.; Graham, S. R.; Ferrence, G. M.; Szczepura, L. F. *Inorg. Chem.* **2003**, *42*, 7326.
(45) Milgrom, L. R.; Zuurbier, R. J.; Gascoyne, J. M.; Thompsett, D.; Moore, B. C. *Polyhedron* **1992**, *11*, 1779.

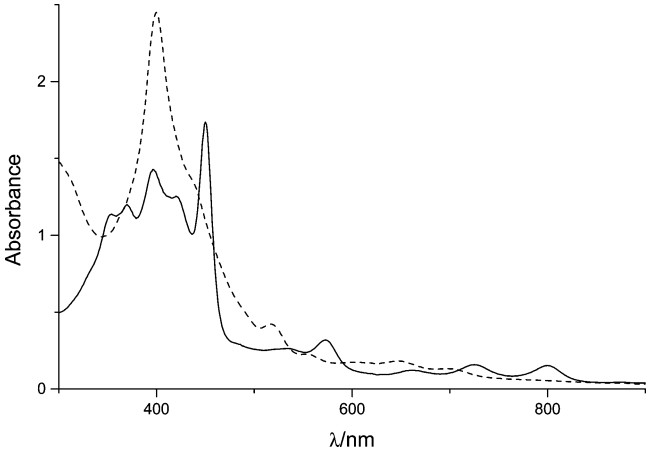

Figure 7. Optical spectrum of **7a** in dichloromethane (solid line) and after addition of 3 equiv of *t*-BuOK (dashed line).

the respective signal in the ^{195}Pt NMR spectrum of benziporphyrin platinum(II) complex (560 ppm)[46] which possesses the same NNNC donor set.

The proton 2-NH can be removed from **7** in a similar way as in the case of **2**,[27] i.e. by application of a strong base. Addition of potassium *tert*-butoxide in THF to the solution of **7** in dichloromethane, toluene, or THF significantly changes the electronic spectrum (Figure 7). The ^{1}H NMR spectrum of **7** after addition of 1 equiv of *t*-BuOK reveals deprotonation of outer nitrogen (2-NH signal near 10 ppm disappears) but also shows features typical of dimeric species, i.e. high-field shift of one of the *meso*-aryl protons to 6.20 and 5.29 ppm (**7b**, CD_2Cl_2, 298 K). Mass spectrometry supports formation of the bis(porphyrinoid) system (*m*/*z* 1768, expected 1768 for [(**7b**)$_2$K] + 1) suggesting potassium cation as a bridge between deprotonated nitrogens of two inverted pyrrole units. At higher concentration of the base (from 2 equiv) all ^{1}H NMR spectral lines broaden likely due to a consecutive equilibrium leading to a monomeric deprotonated species. The signal in the mass spectrum (*m*/*z* 903, expected 903 for [**7b**+K]) suggests replacement of the external 2-NH proton by a potassium ion. An analogous deprotonation process with formation of a dimeric intermediate has been observed previously in the case of **2**, that is the nickel(II) analogue of **7**.[27]

Redox Properties. Coordination to platinum(II) changes the redox properties of the porphyrinoid subunits in **5** and **6** with respect to the starting complexes **3** and **4** (Figure 8). In the cyclic voltammogram of **5** two anodic peaks of irreversible couples appear at 860 and 920 mV (850 and 930 mV for **6**; all potentials are given vs an Ag/AgCl reference electrode); thus the first oxidation potential of **5** is strongly anodically shifted with respect to that of **3** (755 mV; 784 mV for **4**). Since this potential is related to the Ni^{II}/Ni^{III} oxidation process,[29] such a shift indicates a lower accessibility of the +III oxidation state in both subunits of the dimer. It is likely due to the lowering of net electron density on the nickel(II) caused by coordination to the electron withdrawing platinum(II) ion. On the other hand, two

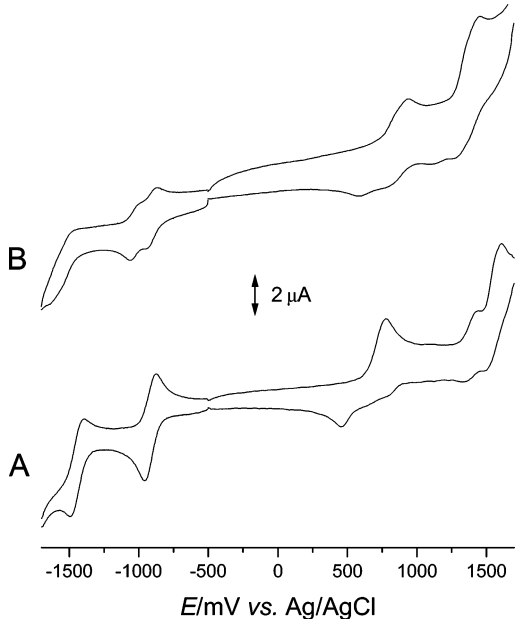

Figure 8. Cyclic voltammograms of **4** (A) and **6** (B) in CH_2Cl_2. Conditions: supporting electrolyte, 0.1 M TBAP; scan rate, 100 mV/s; working electrode, glassy carbon disk; auxiliary electrode, platinum wire; reference electrode, Ag/AgCl (ferrocene reference, 530 mV).

reversible couples (−884 and −990 mV for **5**; −900 and −1032 for **6**), which are related to the reductions of two inequivalent porphyrinoid subunits of the dimer, take place at only slightly different potentials than analogous processes for **3** and **4** (−935 mV and −916 mV, respectively). This is in contrast with the case of protonation of the external nitrogen in **3** or **4**. The first oxidation also takes place at higher potentials in the protonated species, but the reduction of the nickel center occurs at about −400 mV.[29] It may appear that the spin state and/or coordination number of nickel(II) is responsible for its tendency to be reduced to monovalent species. However, reduction on the metal center in the diamagnetic 21-C-protonated complex **2**−TFA takes place at −430 mV.[29] It seems that compensation of the positive charge of Pt^{2+} by the coordinated chloride and deprotonated *ortho*-carbon disfavors reduction of nickel(II) ions in **5** and **6**. The asymmetric character of the dimers and lack of redox data for the appropriate monomeric references prevent discussion concerning the interaction between subunits such as that observed previously for covalently linked bis(carbaporphyrinoids).[28,29]

A cyclic voltammogram of **7a** in dichloromethane consists of one quasi-reversible couple at 803 mV (ΔE_{pp} = 85 mV) and two irreversible waves with potential at 1375 mV (anodic scan) and −1028 mV (cathodic scan). The high anodic and low cathodic potentials indicate that both oxidation and reduction of **7** occur on the ligand rather than on the metal center. Addition of strong base causes cathodic shift of all observed potentials. Most significantly, the couple of the first oxidation appears at 402 mV (ΔE_{pp} = 75 mV) in the presence of 3 equiv of potassium *tert*-butoxide. The irreversible reduction takes place at −1700 mV, while the second oxidation gives an irreversible wave at 980 mV. The first oxidation process can be in this case assigned to the Pt^{2+}/Pt^{3+} pair.

(46) Stępień, M.; Latos-Grażyński, L. *Chem. Eur. J.* **2001**, *7*, 5113.

Apparently, abstraction of the proton from the 2-NH of **7** (vide supra) facilitates a metal-centered oxidation. A similar influence due to deprotonation on the redox properties has been observed for nickel(II)[29] and copper(II)[47] complexes of inverted porphyrin.

A product of chemical oxidation of the platinum(II) center can be detected by EPR in frozen dichloromethane/toluene or THF solutions containing **7**, a 5-fold molar excess of iodine, and 3 equiv of *t*-BuOK. Significantly, there is no EPR signal before addition of the base. The observed spectrum indicates slight orthorhombic and significant axial anisotropy of the Zeeman tensor ($g_1 = 2.260$, $g_2 = 1.991$, $g_3 = 1.985$, CH_2Cl_2/toluene 50/50 v/v, 77 K; $g_1 = 2.210$, $g_2 = 1.997$, $g_3 = 1.990$, THF, 77 K) indicating considerable contribution of metal orbitals to the singly occupied molecular orbital. Lack of the spectral line splitting due to coupling with potential iodide ligand as well as the relation between the principal Zeeman tensor components ($g_{||} > g_{\perp}$) suggest no apical coordination of an anionic ligand. This is in line with four-coordinated character of the trivalent metal center in the environment of trianionic inverted porphyrin.[19,47]

In general, paramagnetic monomeric platinum(III) complexes are very rare[48,49] because trivalent platinum has a strong tendency to dimerization that quenches spins of unpaired electrons.[50] Few examples of paramagnetic mixed-valence $Pt^{II}-Pt^{III}$ species are also known.[51,52] The oxidized **7** seems to have limited stability in solution, since its EPR signal disappears when the solution is stored at room temperature for a few hours.

Conclusions

Formation of an asymmetric dimer by coordination of 21-alkylated nickel(II) complexes of tetraaryl inverted porphyrin is chemo- and diastereoselective. In the described dimeric systems C21 and N2 of both parts of the dimer are fully involved in coordination forming σ-bonds with different metal ions. Studies on the application of the chloroplatinum template in the construction of molecular assemblies of covalently linked inverted porphyrins are in progress.

Experimental Section

Instrumentation. Absorption spectra were recorded on a diode array Hewlett-Packard 8453 spectrometer. Mass spectra were recorded on an AD-604 spectrometer using the electrospray and electron impact techniques and Voyager-Elite spectrometer for MALDI TOF spectra using a matrix of 2,5-dihydroxybenzoic acid and 337 nm laser radiation pulses. NMR spectra were recorded on a Bruker Avance 500 spectrometer. The 1D and 2D experiments (COSY, NOESY, ROESY, HMQC, and HMBC) were performed by means of standard experimental procedures of the Bruker library. The peaks were referenced to the residual $CHCl_3$ resonances in ^1H and ^{13}C NMR (7.24 and 77.2 ppm, respectively) and to external [Pt(TPP)] in $CDCl_3$[45] (1235 ppm, Ξ-scale) in the case of ^{195}Pt. Cyclovoltammetric measurements were performed in dichloromethane on an EA9C MTM apparatus with a glassy carbon disk as the working electrode, Ag/AgCl as the reference electrode (ferrocene reference potential was 530 mV), and platinum wire as the auxiliary electrode. Tetrabutylammonium perchlorate (0.1 M) was used as the supporting electrolyte.

EPR spectra were obtained with a Bruker ESP 300E spectrometer. The magnetic field was calibrated with a proton magnetometer and EPR standards. The EPR spectra were simulated by assuming orthorhombic symmetry. The details of the EPR simulations have been given elsewhere.[53−55]

Preparation of Samples. Dichloromethane-d_2 and chloroform-*d* used for NMR samples were passed through basic alumina before use. The samples of **7** for NMR or spectrophotometric titration with potassium *tert*-butoxide were prepared in the inert atmosphere of a glovebox. A solution of *t*-BuOK in THF was added by syringe to the NMR tube or quartz spectrophotometric cell containing a solution of **7** in dichloromethane and sealed with silicon septa.

Preparation of Precursors. 5,10,15,20-Tetraphenyl-2-aza-21-carbaporphyrin, 5,10,15,20-tetrakis(*p*-tolyl)-2-aza-21-carbaporphyrin (**1**), and their nickel(II) complexes (**2**) were synthesized according to known procedures.[12,56] Syntheses of complexes **3** and **4** were described previously.[18,29]

Syntheses of Dimers. In a typical synthesis 30 mg of **3** or **4** was refluxed for 24 h in $CHCl_3$ (30 mL) with a suspension of 20 mg of $PtCl_2$ and 20 mg of K_2CO_3 under a blanket of nitrogen. Flash chromatography on silica gel with benzene allows the separation of reaction products **5** or **6** from the respective residual starting material (fastest migrating band). Yields (crystallized from benzene/hexane): **5**, 23 mg, (66%); **6**, 20 mg, (62%).

Selected data for **5**: $\lambda_{max}(CH_2Cl_2)$/nm (log ϵ) 293 (4.82), 356 (4.79), 436 (5.02), 513 sh, 616 sh, 768 sh. MS (MALDI) calcd for $C_{98}H_{75}N_8Ni_2PtCl$: 1712.6. Found: 1713 ($[M]^+$), 1677 ($[M - Cl]^+$). Anal. Calcd for $C_{98}H_{75}N_8Ni_2PtCl$: C, 68.79; H, 4.39; N, 6.55. Found: C, 68.50; H, 4.53; N, 6.30. ^1H NMR (500 MHz, $CDCl_3$, 213 K): $\delta_H = 10.26$ (s, 1H), 9.19 (d, 4.6 Hz, 1H), 8.77 (d, 4.6 Hz, 1H), 8.69 (d, 4.6 Hz, 1H), 8.66 (d, 4.6 Hz, 1H), 8.53 (d, 5.0 Hz, 1H), 8.57 (d, 4.6 Hz, 1H), 8.56 (d, 4.6 Hz, 1H), 8.47 (d, 7.3 Hz, 1H), 8.36 (d, 5.0 Hz, 1H), 8.34 (d, 5.0 Hz, 1H), 8.28 (d, 0.9 Hz, 1H), 8.24 (d, 7.8 Hz, 1H), 8.11 (d, 8.2 Hz, 1H), 8.09 (d, 8.7 Hz, 1H), 7.97 (d, 6.4 Hz, 1H), 7.96 (d, 6.9 Hz, 1H), 7.88 (d, 7.4 Hz, 1H), 7.85 (d, 4.6 Hz, 1H), 7.82 (d, 7.4 Hz, 1H), 7.77 (d, 7.3 Hz, 1H), 7.75 (d, 7.3 Hz, 1H), 7.69 (d, 7.4 Hz, 1H), 7.67 (d, 9.1 Hz, 1H), 7.61 (d, 6.4 Hz, 1H), 7.59 (d, 7.8 Hz, 1H), 7.55 (d, 6.4 Hz, 1H), 7.53 (d, 6.9 Hz, 1H), 7.51 (d, 7.8 Hz, 1H), 7.46 (d, 7.3 Hz, 1H), 7.42 (d, 7.8 Hz, 1H), 7.39 (d, 8.2 Hz, 1H), 7.20 (d, 9.1 Hz, 1H), 7.18 (d, 6.8 Hz, 1H), 7.14 (d, 5.0 Hz, 1H), 7.06 (d, 7.8 Hz, 1H), 6.84 (d, 7.8 Hz, 1H), 6.76 (d, 5.0 Hz, 1H), 6.39 (d, 7.3 Hz, 1H), 6.04 (d, 7.3 Hz, 1H), 4.99 (d, 7.3 Hz, 1H), 4.49 (s, 1H), 4.39 (d, 7.3 Hz, 1H), 3.87 (d, 7.3 Hz, 1H), 3.52 (d, 7.3 Hz, 1H), 2.72 (s, 3H), 2.69 (s, 3H), 2.68 (s, 3H), 2.67 (s, 3H), 2.40 (s, 3H), 1.93 (s, 3H), 1.22 (s, 3H), −3.09 (s, 3H), −3.18 (s, 3H). ^{13}C NMR (125 MHz, $CDCl_3$, 213 K, partial data): $\delta_C = 173.0$ (1′), 164.8 (1),

(47) Maeda, H.; Ishikawa, Y.; Matsuda, T.; Osuka, A.; Furuta, H. *J. Am. Chem. Soc.* **2003**, *125*, 11822.
(48) Uson, R.; Fornies, J.; Tomas, M.; Menjon, B.; Suenkel, K.; Bau, R. *Chem. Commun.* **1984**, *1984*, 751.
(49) Uson, R.; Fornies, J.; Tomas, M.; Menjon, B.; Bau, R.; Suenkel, K.; Kuwabara, E. *Organometallics* **1986**, *5*, 1576.
(50) Lippert, B. *Coord.Chem.Rev.* **1999**, *182*, 263 and references therein.
(51) Arrizabalaga, P.; Castan, P.; Geoffroy, M.; Laurent, J.-P. *Inorg. Chem.* **1985**, *24*, 3656.
(52) Peilert, M.; Erxleben, A.; Lippert, B. *Z. Anorg. Allg. Chem.* **1996**, *622*, 267.
(53) Chmielewski, P. J.; Grzeszczuk, M.; Latos-Grażyński, L.; Lisowski, J. *Inorg. Chem.* **1989**, *28*, 3546.
(54) Chmielewski, P. J.; Latos-Grażyński, L.; Pacholska, E. *Inorg. Chem.* **1994**, *33*, 1992.
(55) Chmielewski, P. J.; Latos-Grażyński, L. *Inorg. Chem.* **1997**, *36*, 840.
(56) Geier, G. R., III; Haynes, D. M.; Lindsey, J. S. *Org. Lett.* **1999**, *1*, 1455.

152.1 (3′), 151.6 (4′), 150.2 (4), 140.5 (20m$_1$), 139.5 (3), 137.7, 136.4, 136.2, 135.2, 134.9, 134.6, 134.3, 134.3, 134.2, 134.0, 133.9, 133.8, 133.7, 133.7, 133.7, 133.5, 133.4, 133.2, 133.1, 133.0, 132.9, 132.8, 132.8, 132.1, 132.0, 131.7, 131.6, 130.0, 128.3, 128.1, 128.0, 127.9, 127.9, 127.8, 127.4, 126.9, 126.3, 125.8, 125.7, 31.8 (21′), 23.9 (21), 22.3, 21.9, 21.8, 21.7, 21.6, 21.5, 21.2, 20.2, 16.1 (21′-Me), 15.5 (21-Me).

Selected data for **6**: $\lambda_{max}(CH_2Cl_2)$/nm (log ϵ) 294 (4.81), 363 (4.79), 440 (5.03), 524 sh, 625 sh, 766 sh. MS (MALDI-TOF) calcd for $C_{110}H_{83}N_8Ni_2PtCl$: 1864. Found: 1864 ([M]$^+$), 1829 ([M − Cl]$^+$), 1774 ([M − Bz]$^+$), 1739 ([M − Bz − Cl]$^+$), 1682 ([M − 2Bz]$^+$), 1647 ([M − 2Bz − Cl]$^+$). ^{1}H NMR (500 MHz, $CDCl_3$, 233 K): δ_H = 10.07 (s, 1H), 9.22 (d, 4.8 Hz, 1H), 8.75 (d, 4.6 Hz, 1H), 8.70 (d, 4.6 Hz, 1H), 8.65 (d, 4.8 Hz, 1H), 8.60 (d, 4.6 Hz, 1H), 8.55 (d, 4.6 Hz, 2H), 8.41 (d, 4.6 Hz, 1H), 8.40 (d, 4.6 Hz, 1H), 8.30 (d, 8.0 Hz, 1H), 8.28 (d, 1.0 Hz, 1H), 8.11 (d, 7.6 Hz, 1H), 8.05 (d, 7.4 Hz, 1H), 7.94 (d, 4.6 Hz, 1H), 7.92 (d, 7.3 Hz, 1H), 7.90 (d, 8.0 Hz, 1H), 7.88 (d, 7.3 Hz, 1H), 7.78 (d, 7.3 Hz, 1H), 7.72 (d, 8.0 Hz, 1H), 7.61 (d, 7.3 Hz, 1H), 7.59 (d, 7.3 Hz, 1H), 7.56 (d, 7.3 Hz, 1H), 7.54 (d, 6.8 Hz, 2H), 7.47 (d, 7.6 Hz, 1H), 7.42 (d, 7.6 Hz, 1H), 7.40 (d, 7.6 Hz, 1H), 7.27 (d, 7.4 Hz, 1H), 7.19 (d, 5.0 Hz, 1H), 7.17 (d, 7.3 Hz, 1H), 7.05 (d, 7.6 Hz, 1H), 6.93 (d, 4.8 Hz, 1H), 6.81 (m, 1H), 6.72 (m, 2H), 6.33 (m, 1H), 6.11 (m, 2H), 5.55 (d, 7.3 Hz, 1H), 5.15 (d, 7.1 Hz, 1H), 5.08 (d, 7.5 Hz, 2H), 4.82 (d, 7.6 Hz, 1H), 4.63 (d, 7.6 Hz, 2H), 4.35 (d, 7.1 Hz, 1H), 3.95 (d, 6.7 Hz, 1H), 3.91 (s, 1H), 3.63 (d, 7.1 Hz, 1H), 2.73 (s, 3H), 2.70 (s, 3H), 2.68 (s, 3H), 2.67 (s, 3H), 2.62 (s, 3H), 2.43 (s, 3H), 1.92 (s, 3H), 1.06 (s, 3H), −0.97 (d, 14.9 Hz, 1H), −0.98 (d, 14.4 Hz, 1H), −1.63 (d, 14.2 Hz, 1H), −2.00 (d, 14.9 Hz, 1H). ^{13}C NMR (125 MHz, $CDCl_3$, 233 K, partial data): δ_C = 170.6 (1′), 162.5 (1), 155.1 (3′), 154.9, 152.6, 151.7, 151.0, 150.8, 150.5, 149.9, 148.7, 148.6, 148.0, 147.9, 147.7, 141.1, 140.9, 140.0 (3), 139.4, 138.3, 138.2, 138.1, 138.0, 137.9, 137.8, 137.7, 137.6, 137.4, 137.2, 136.6, 136.5, 136.4, 136.2, 136.0, 135.4, 134.8, 134.5, 134.3, 134.0, 133.9, 133.6, 133.5, 133.4, 133.3, 133.2, 133.1, 132.9, 132.6, 132.3, 132.2, 132.1, 131.7, 129.4, 128.6, 128.0, 127.9, 127.8, 127.7, 127.6, 127.3, 126.4, 126.3, 126.2, 126.1, 125.8, 125.7, 125.4, 125.1, 39.9 (21′), 35.3 (21′-*C*H$_2$), 34.4 (21-*C*H$_2$), 31.1 (21), 21.8, 21.7, 21.6, 21.4, 20.0.

Syntheses of 5,10,15,20-Tetraphenyl-2-aza-21-carbaporphyrinatoplatinum(II), 7a, and 5,10,15,20-Tetrakis-(*p*-tolyl)-2-aza-21-carbaporphyrinatoplatinum(II), 7b. A solution containing 20 mg (0.03 mmol) of **1** and 70 mg (0.15 mmol) of $Pt(PhCN)_2Cl_2$ in chlorobenzene (50 mL) was refluxed for 6 h. The solvent was then removed, and the product was chromatographed with benzene on a silica gel column. The fastest moving red band contained **7**. Crystallization from benzene/hexane gave 17 mg of the product in the case of **7a** (yield 70%) and 15 mg in the case of **7b** (60%).

Selected data for **7a**: $\lambda_{max}(CH_2Cl_2)$/nm (log ϵ) 350 sh, 368 (4.68), 395 (4.76), 417 (4.76), 447 (4.87), 527 (3.98), 565 (4.04), 651 (3.56), 711 (3.71), 783 (3.68). HR-MS (ESI) calcd for $C_{44}H_{28}N_4Pt$: 807.1962. Found: 807.1956 ([M]$^+$). ^{1}H NMR (500 MHz, $CDCl_3$, 333 K): δ_H = 9.78 (1H, s, 2-NH), 8.11 (1H, m, $^3J_{HH}$ = 3.7 Hz, $^4J_{PtH}$ = 8.9 Hz, 3), 7.91 (2H, m), 7.89 (2H, m), 7.88−7.81 (8H, overlapping multiplets), 7.78 (1H, d, J = 4.9 Hz), 7.73 (1H, d, J = 4.9 Hz), 7.72 (1H, d, J = 4.9 Hz), 7.71 (1H, d, J = 5.2 Hz), 7.65−7.61(3H, m), 7.58−7.52 (10H, overlapping multiplets). ^{13}C NMR (125 MHz, $CDCl_3$, 333 K, partial data): δ_C = 152.3, 149.2, 141.2, 141.7, 147.9, 140.0, 133.2, 133.4, 132.6, 132.1, 131.5, 130.6, 130.5, 128.8, 128.2, 128.3, 127.6, 127.5, 127.3, 127.2, 126.8, 125.5, 122.6.

Selected data for **7b**: $\lambda_{max}(CH_2Cl_2)$/nm (log ϵ) 234 (4.61), 351 sh, 367 (4.69), 394 (4.78), 416 (4.76), 446 (4.87), 527 (3.99), 565 (4.03), 653 (3.56), 711 (3.72), 782 (3.69). HR-MS (ESI) calcd for $C_{48}H_{36}N_4Pt$: 863.2588. Found: 863.2601 ([M]$^+$). Anal. Calcd for $C_{48}H_{36}N_4Pt$: C, 66.73; H, 4.20; N, 6.49. Found: C, 66.95; H, 4.44; N, 6.52. ^{1}H NMR (500 MHz, $CDCl_3$, 298 K): δ_H = 9.81 (1H, s, 2-NH), 8.12 (1H, m, $^3J_{HH}$ = 4.0 Hz, $^4J_{PtH}$ = 8.5 Hz, 3), 7.88 (1H, d, J = 5.2 Hz), 7.86 (1H, d, J = 5.5 Hz), 7.81 (1H, d, J = 5.2 Hz), 7.77−7.68 (10H, overlapping multiplets), 7.42 (2H, m), 7.38 (6H, m), 2.56 (9H, s), 2.55 (3H, s).^{13}C NMR (125 MHz, $CDCl_3$, 333 K, partial data): δ_C = 152.9, 150.2 (3-C), 149.7, 140.8, 139.5, 137.7, 135.3, 134.3, 133.8, 133.7, 133.6, 132.0, 129.6, 129.1, 128.6, 128.5, 127.9, 126.8, 123.2, 123.5, 120.7, 119.4, 22.4.

Table 1. Crystal Data and Structure Refinement for **6**·C_6H_6

empirical formula	$C_{116}H_{89}N_8ClNi_2Pt$
fw	1942.91
temp	100(2) K
wavelength	0.71073 Å
crystal system	monoclinic
space group	*C*2/*c*
unit cell dimens	
a	22.8081(16) Å
b	27.075(2) Å
c	30.787(2) Å
α	90°
β	103.255(6)°
γ	90°
volume	18505(2) Å^3
Z	8
density (calcd)	1.395 Mg/m^3
absorption coeff	1.996 mm^{-1}
F(000)	7936
crystal size	0.10 × 0.07 × 0.05 mm^3
crystal color and habit	brown block
diffractometer	Kuma KM4CCD
θ range for data collection	3.12−28.55°
index ranges	$-30 \le h \le 30$, $-35 \le k \le 36$, $-41 \le l \le 28$
reflns collected	63948
indep reflns	21799
completeness to θ = 28.55°	92.4%
absorption correction	analytical
max and min transmission	0.9068 and 0.8254
solution method	SHELXS-97 (Sheldrick, 1990)
refinement method	full-matrix least-squares on F^2
data/restraints/params	21799/0/535
GOF on F^2	1.069
final *R* indices [$I > 2\sigma(I)$][a]	R1 = 0.1434, wR2 = 0.2121
R indices (all data)[a]	R1 = 0.3302, wR2 = 0.2737
largest diff peak and hole	1.034 and −1.532 e Å^{-3}

[a] $R1 = \sum||F_o| - |F_c||/\sum|F_o|$, $wR2 = [\sum[w(F_o^2 - F_c^2)^2/\sum[w(F_o^2)^2]]^{1/2}$.

X-ray Data Collection and Refinement of 6. Crystals of **6**·C_6H_6 were prepared by diffusion of *n*-hexane into the benzene solution contained in a thin tube. Data were collected at 100 K using an Oxford Cryosystem device on a Kuma KM4 κ-axis diffractometer with graphite-monochromated Mo Kα radiation and CCD detector. Data collection, integration and scaling of the reflections, and analytical absorption correction were performed by means of the CrysAlis suite of programs.[57] Crystal data are compiled in Table 1. The structure was solved by direct methods with SHELXS97[58] and refined by the full-matrix least-squares method on all F^2 data using SHELXL97[59] programs. Only platinum, nickel, and chlorine atoms were refined with anisotropic displacement parameters; hydrogen atoms were included from geometry

(57) Oxford Diffraction 2001, CrysAlis "CCD" and CrysAlis "RED", Oxford Diffraction (Poland) Sp. z o.o., Wrocław, Poland. 2001.
(58) Sheldrick, G. M. *SHELXS97—Program for Crystal Structure Solution*; University of Göttingen: Göttingen, 1997.
(59) Sheldrick, G. M. *SHELXL97—Program for Crystal Structure Refinement*; University of Göttingen: Göttingen, 1997.

of molecules. The asymmetric unit contains **6**, one molecule of benzene, and a half of a disordered hexane molecule. The original reflection data were processed with the SQUEEZE procedure included in the PLATON[60] suite in order to determine the void regions potentially occupied by solvents (1466.5 $Å^3$) and a total of 124 electrons/cell were recovered. Final cycles of refinement were performed on the hexane-free reflection data.

Acknowledgment. This work was supported by the State Committee for Scientific Research of Poland (Grant 7 T09A 120 20 and 3 09A 155 15).

Supporting Information Available: Crystallographic data of **6** in CIF format. NOESY spectrum for **5**, scheme showing interprotonic contacts for **5**, ^1H NMR spectra of **7b** and its deprotonated form, cyclic voltammograms for **7b** and its deprotonated form, and EPR spectrum of oxidized **7a.** This material is available free of charge via the Internet at http://pubs.acs.org.

IC035162L

(60) Spek, A. L. PLATON, A Multipurpose Crystallographic Tool. *Acta Crystallogr., Sect. A* **1990**, *46*, C-34.